The use of microperforated plates to attenuate cavity resonances

Fenech, Benjamin; Keith, Graeme; Jacobsen, Finn

Published in:
Acoustical Society of America. Journal

Link to article, DOI:
10.1121/1.2258438

Publication date:
2006

Document Version
Publisher's PDF, also known as Version of record

The use of microperforated plates to attenuate cavity resonances

Benjamin Fenech[a)]
Acoustic Technology, Ørsted·DTU, Technical University of Denmark, Building 352, Ørsteds Plads, DK-2800 Kgs. Lyngby, Denmark

Graeme M. Keith[b)]
Ødegaard & Danneskiold-Samsøe, Titangade 15, DK-2200 Copenhagen N, Denmark

Finn Jacobsen[c)]
Acoustic Technology, Ørsted·DTU, Technical University of Denmark, Building 352, Ørsteds Plads, DK-2800 Kgs. Lyngby, Denmark

(Received 31 October 2005; revised 30 June 2006; accepted 3 July 2006)

The use of microperforated plates to introduce damping in a closed cavity is examined. By placing a microperforated plate well inside the cavity instead of near a wall as traditionally done in room acoustics, high attenuation can be obtained for specific acoustic modes, compared with the lower attenuation that can be obtained in a broad frequency range with the conventional position of the plate. An analytical method for predicting the attenuation is presented. The method involves finding complex eigenvalues and eigenfunctions for the modified cavity and makes it possible to predict Green's functions. The results, which are validated experimentally, show that a microperforated plate can provide substantial attenuation of modes in a cavity. One possible application of these findings is the treatment of boiler tones in heat-exchanger cavities. © *2006 Acoustical Society of America.* [DOI: 10.1121/1.2258438]

PACS number(s): 43.20.Hq, 43.50.Gf [RR] Pages: 1851–1858

I. INTRODUCTION

For a number of years, microperforated plates have been used as an alternative to fibrous absorptive materials to provide absorption at the boundary surfaces to acoustic cavities. Microperforated plates are particularly well suited to applications requiring tolerance to high temperatures, such as the heat exchanger cavities of boilers, and sterile environments where the introduction of small fibrous particles is unacceptable.

Traditionally, the plates are located a fixed distance from the wall of the cavity and their acoustic characteristics are described in terms of the reflection and absorption of incoming acoustic waves at the plate. This approach is particularly effective at high frequencies where a large number of modes play a significant role in the acoustic behavior of the cavity, and the direction of the incoming waves on the plate can be thought of as being distributed in an almost continuous way, in other words, when the sound field is diffuse.

There are, however, several applications that require attenuation at low frequencies where the acoustic response is dominated by a handful of well-separated modes. One such application is the treatment of so-called boiler tones.[1,2] These are generated by an unstable interaction between the acoustic response to the excitation caused by unsteady flow and the unsteady flow itself and can lead to extremely high levels of tonal noise at even fairly modest flow speeds. Tones can be identified with particular individual acoustic eigenmodes, and the problem is to find a method of increasing the attenuation of a given mode, or a handful of selected modes, rather than to increase the attenuation across a broad range of frequencies.

In these situations, much greater levels of attenuation can be achieved by locating the microperforated plate at some point well inside the cavity. Wherever the plate is located, an accurate analysis of the acoustic characteristics of the plate in the cavity at low frequencies must take account of the modal structure of the cavity. A local analysis at the plate surface is no longer adequate because the "incident" and "reflected" waves are strongly linked through the boundary conditions at the walls of the cavity. The problem becomes essentially a complex eigenvalue problem.

In using microperforated plates in this way to attenuate specific low frequency modes in a cavity, there are two key practical questions that need to be addressed: "What is the optimal location of the plates?" and "What is the flow impedance of the plate that provides the optimal attenuation?" Obviously, such optimization requires a reliable model for predicting the effect of the plates. This paper focuses on the development and validation of such a model. Thus, a theoretical paradigm is presented, a simple analytical model based on this paradigm is derived, and the results of an experimental test of the validity of this model are presented.

II. OUTLINE OF THEORY

A. Boundary conditions and power loss

Consider a volume Ω divided into two subvolumes Ω^+ and Ω^- by a perforated plate lying on a surface Π. At each

[a)]Author to whom correspondence should be addressed. Current affiliation: Aerodynamics & Flight Mechanics Research Group, School of Engineering Sciences, University of Southampton, Southampton, SO17 1BJ, United Kingdom. Electronic mail: bfenech@gmail.com
[b)]Electronic mail: gk@oedan.dk
[c)]Electronic mail: fja@oersted.dtu.dk

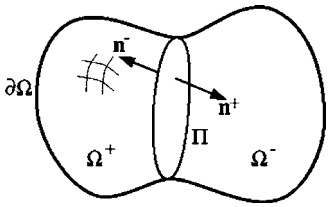

FIG. 1. A volume Ω with boundary $\partial\Omega$ divided by a perforated plate on the surface Π into two subvolumes Ω^+ and Ω^- with outward pointing normals $\mathbf{n}^+$ and $\mathbf{n}^-$.

point $\mathbf{x}_\Pi$ on the plate, the unit vectors $\mathbf{n}^+$ and $\mathbf{n}^-$ are normal to Π and are such that $\mathbf{n}^+$ (respectively, $\mathbf{n}^-$) points out of Ω^+ (respectively, Ω^-); see Fig. 1.

The plate is taken to be sufficiently thin that compressibility effects inside the plate may be neglected. Denoting by $\mathbf{u}^+(\mathbf{x}_\Pi)$ and $\mathbf{u}^-(\mathbf{x}_\Pi)$ the acoustic particle velocities on the two sides of the plate at the point $\mathbf{x}_\Pi \subset \Pi$ continuity of mass gives

$$\mathbf{u}^+(\mathbf{x}_\Pi)\cdot\mathbf{n}^+(\mathbf{x}_\Pi) = \mathbf{u}^-(\mathbf{x}_\Pi)\cdot\mathbf{n}^+(\mathbf{x}_\Pi) = -\mathbf{u}^-(\mathbf{x}_\Pi)\cdot\mathbf{n}^-(\mathbf{x}_\Pi). \tag{1}$$

Viscous losses in the plate support a pressure discontinuity across the surface Π. In the linear limit, this pressure difference is taken to be proportional to the component of the acoustic particle velocity normal to the surface. Denoting by $p^+(\mathbf{x}_\Pi)$ and $p^-(\mathbf{x}_\Pi)$ the pressures on the two sides of the plate at the point $\mathbf{x}_\Pi$, we have

$$p^+(\mathbf{x}_\Pi) - p^-(\mathbf{x}_\Pi) = R(\omega)\mathbf{u}^+(\mathbf{x}_\Pi)\cdot\mathbf{n}^+(\mathbf{x}_\Pi), \tag{2}$$

where $R(\omega)$ is the flow impedance, which is typically a complex valued function of the frequency ω.

The Fourier transform of the linearized Euler momentum equation gives a relation between the acoustic particle velocity and the gradient of the pressure,

$$\nabla p = i\omega\rho_0\mathbf{u} \tag{3}$$

(in which ρ_0 is the density of the medium), and turns the plate conditions given by Eqs. (1) and (2) into conditions involving only the pressure and its gradient,

$$\nabla p^+(\mathbf{x}_\Pi)\cdot\mathbf{n}^+(\mathbf{x}_\Pi) = -\nabla p^-(\mathbf{x}_\Pi)\cdot\mathbf{n}^-(\mathbf{x}_\Pi), \tag{4}$$

$$p^+(\mathbf{x}_\Pi) - p^-(\mathbf{x}_\Pi) = \frac{R(\omega)}{\rho_0 c_0}\frac{1}{ik_0}\nabla p^+(\mathbf{x}_\Pi)\cdot\mathbf{n}^+(\mathbf{x}_\Pi), \tag{5}$$

where c_0 is the speed of sound and $k_0 = \omega/c_0$ is the wave number. For a given pressure field $p(\mathbf{x},\omega)$ inside the volume Ω the time averaged sound power dissipated by the perforated plate is given by

$$P_d(\omega) = \frac{1}{2}\Re\left\{\int_\Pi [p^{+*}(\mathbf{x},\omega)\mathbf{u}^+(\mathbf{x},\omega)\cdot\mathbf{n}^+ + \mathbf{p}^{-*}(\mathbf{x},\omega)\mathbf{u}^-(\mathbf{x},\omega)\cdot\mathbf{n}^-]\mathrm{d}^2\mathbf{x}\right\}, \tag{6}$$

which with Eqs. (1) and (2) can be written

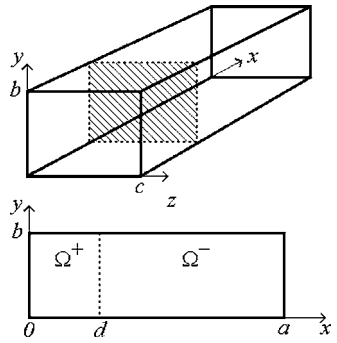

FIG. 2. A rectangular prism with a perforated plate.

$$P_d(\omega) = \frac{1}{2}\Re\{R(\omega)\}\int_\Pi |\mathbf{u}^+\cdot\mathbf{n}^+|^2\mathrm{d}^2\mathbf{x}. \tag{7}$$

Thus the dissipated power is proportional to the real part of the flow impedance and the square of the magnitude of the normal component of the velocity at the plate surface, averaged over the plate. Clearly if the real part of the flow impedance is zero then there is no dissipation. On the other hand, if the real part of the flow impedance is too great then the plate becomes effectively impenetrable, the normal component of the velocity through the plate is zero, and there is no dissipation. Between these two extremes there is an optimal flow impedance, the determination of which requires further knowledge of the pressure field inside the cavity.

All the standard results regarding the acoustics of closed cavities with losses follow.[3] In particular there exists a complete set of orthogonal eigenfunctions $\xi_n(\mathbf{x},\omega)$ with corresponding eigenvalues $\kappa_n(\omega)$ such that

$$(\nabla^2 + \kappa_n^2)\xi_n = 0, \tag{8}$$

subject to the boundary conditions given by Eqs. (4) and (5). Note that due to the frequency dependence of the boundary condition, the eigenvalues and eigenfunctions will in general be functions of the (real) frequency ω. Any given pressure field in Ω can be written as a weighted sum of the eigenfunctions. In particular, the Green's function for the cavity, which satisfies

$$(\nabla^2 + k_0^2)G(\mathbf{x},\mathbf{y};\omega) = -\delta(\mathbf{x}-\mathbf{y}), \tag{9}$$

is given by[3]

$$G(\mathbf{x},\mathbf{y};\omega) = -\sum_{n=1}^{\infty}\frac{\xi_n(\mathbf{x})\xi_n(\mathbf{y})}{V[k_0^2 - \kappa_n^2(\omega)]}, \tag{10}$$

where $\mathbf{x}$ and $\mathbf{y}$ are the source and receiver positions, respectively.

B. A one-dimensional eigenvalue problem

The simplest problem involving a cavity and a perforated plate is that of a rectangular enclosure with the plate located perpendicular to one of the axes; see Fig. 2. This problem can be solved by separation of variables, and since the solutions in the two directions parallel to the plate are trivial the problem essentially reduces to the one-dimensional eigenvalue problem

$$X_l''(x) + \alpha_l^2 X_l(x) = 0, \tag{11}$$

subject to hard walled boundary conditions at the ends of the cavity, viz. $X_l'(0)=X_l'(a)=0$, and the one-dimensional equivalents of Eqs. (4) and (5)

$$X_l'(d^-) = X_l'(d^+), \tag{12}$$

$$X_l(d^-) - X_l(d^+) = \frac{R(\omega)}{\rho_0 c_0}\frac{1}{ik_0}X_l'(d^+). \tag{13}$$

It is convenient to introduce the nondimensional variables

$$\bar{x} = x/a, \quad \delta = d/a, \quad \bar{\alpha} = \alpha a, \quad \varpi = \omega a/c_0, \qquad \bar{R} = R/(\rho_0 c_0). \tag{14}$$

Eigensolutions that satisfy the end boundary conditions can be written

$$X(\bar{x}) = \begin{cases} A\cos[\bar{\alpha}\bar{x}] & \bar{x} < \delta, \\ B\cos[\bar{\alpha}(1-\bar{x})] & \bar{x} > \delta, \end{cases} \tag{15}$$

and the first plate condition, Eq. (12), gives

$$A\sin[\delta\bar{\alpha}] + B\sin[(1-\delta)\bar{\alpha}] = 0. \tag{16}$$

Clearly Eq. (16) is satisfied if both $\sin[\delta\bar{\alpha}]$ and $\sin[(1-\delta)\bar{\alpha}]$ are zero. In this case, it can easily be shown that $\sin[\bar{\alpha}]$ is also zero. These modes correspond to the eigenmodes with no plate present that have zero particle velocity at the location of the plate and thus automatically satisfy both plate conditions. If i and j are integers such that i/j is a fraction in its lowest terms and $i/j=\delta/(1-\delta)$, then $\bar{\alpha}_l=l\pi$ with $l=m(i+j)$ and $m=1,2,3\ldots$, are eigenvalues with eigenfunctions

$$X_l(x) = \sqrt{2}\cos(\bar{\alpha}_l\bar{x}) \tag{17}$$

that automatically satisfy both plate conditions.

The second plate condition, Eq. (13), together with Eq. (16), give the following eigenvalue equation for $\bar{\alpha}$:

$$i\sin[\bar{\alpha}] + \frac{\bar{R}}{\varpi}\bar{\alpha}\sin[\delta\bar{\alpha}]\sin[(1-\delta)\bar{\alpha}] = 0. \tag{18}$$

This equation has been solved for $\bar{\alpha}$ by Newton-Raphson iteration, using the set of eigenvalues corresponding to the case with no plate as starting guesses. Since the ratio $\bar{R}/\varpi$ depends on the frequency a solution strategy was developed that involved tracking each eigenvalue as a function of the ratio from the no-plate case, zero, to its value at the corresponding frequency. The number of intermediate values of the ratio was determined by requiring the change in the eigenvalue corresponding to a change in the ratio not to exceed a specified limit. With tolerances appropriately chosen, this method proved to be extremely robust and remarkably fast. Note that this method does not make any requirement of the ordering of the eigenvalues for a finite flow impedance, as the eigenvalues may (and indeed do) swap places in a list ordered by the size of the real part.

C. The analytical model used for comparison with experiments

The method described in the preceding section furnishes a set of eigenvalues that map continuously to the eigenvalues of the zero flow impedance case. Returning now to dimensional notation, the eigenvalues with the plate can be written $\alpha_l=\bar{\alpha}_l/a$. If l is an integer multiple of $(i+j)$, where i and j are integers with no common factors such that $i/j=\delta/(1-\delta)$, then the zero flow impedance eigenfunction automatically satisfies the plate conditions $\alpha_l=\alpha_{l,0}=l\pi/a$ and the eigenfunction is given by Eq. (17). Otherwise, the eigenfunctions can be written

$$X_l(x) = \begin{cases} -\Lambda_l\sin[(1-\delta)\alpha_l a]\cos[\alpha_l x] & x < d, \\ \Lambda_l\sin[\delta\alpha_l a]\cos[\alpha_l(a-x)] & x > d, \end{cases} \tag{19}$$

where Λ_l is a normalizing factor defined by

$$\int_0^a X_l^2(x)dx = a. \tag{20}$$

Consider now the acoustic cavity shown in Fig. 2 with dimensions a, b, and c. It is trivial to show that eigenfunctions of the Helmholtz equation in such a cavity are given by

$$\xi_{l,m,n}(\mathbf{x}) = X_l(x)Y_m(y)Z_n(z), \tag{21}$$

where $Y_m(y)=\sqrt{2}\cos(\beta_m y)$ with $\beta_m=m\pi/b$ for $m\geq 1$, and $Z_n(z)=\sqrt{2}\cos(\gamma_n z)$ with $\gamma_n=n\pi/c$ for $n\geq 1$. The corresponding eigenvalues are given by

$$\kappa_{lmn}^2 = \alpha_l^2 + \beta_m^2 + \gamma_n^2. \tag{22}$$

For one or more of l, m, or n equal to zero, the corresponding eigenfunctions X_0, Y_0, and Z_0 are unity.

The resulting eigenfunctions may be divided into axial, tangential, and oblique modes in the usual manner. The only modes that are not affected by the presence of the perforated plate are modes which, in the absence of the plate, have zero particle velocity in the x direction at the position of the plate. These include modes with wave motion only in the direction parallel to the plate. An axial mode in the y direction, for example, will not be affected by the presence of the plate.

In the limit of an infinite flow impedance of the plate the eigenmode structure tends to the eigenmode structure of two independent cavities, as one would expect. For each mode in, say, the left subcavity the corresponding mode in the combined cavity is equal to the mode in the left subcavity and identically zero in the right subcavity. Such a mode satisfies the boundary conditions and the governing equations everywhere and has a real-valued eigenfrequency equal to the eigenfrequency of the mode in the left subcavity. With a source in, say, the left subcavity the Green's function is zero if the receiver position is in the right subcavity because all modes that are nonzero in the left subcavity are identically zero in the right subcavity.

Using the eigenfunctions given by Eq. (21) in Eq. (10), the analytical model has been compared with numerical (finite element) calculations performed using the commercial finite element code ACTRAN, and the results were found to be virtually indistinguishable. This showed that the analytical solution provides a solution of the Helmholtz equation sub-

ject to the appropriate boundary and plate conditions [Eqs. (4) and (5)]. In Sec. III B it is investigated through a series of experiments whether these boundary and plate conditions are a reasonable model for the behavior of real perforated plates in a real cavity.

III. EXPERIMENTAL VERIFICATION

A. The flow impedance of a microperforated plate

Microperforated plates are available in various formats, ranging from thin transparent films that can be mounted in front of windows to much more robust metal plates for use at high temperatures or in other harsh environments. Many manufacturers offer microperforated plates as a complete acoustic absorber package (i.e., a perforated plate mounted at a certain distance from some rigid backing). A few others offer individual plates, giving much more flexibility to the noise control engineer.

A plate with the required dimensions was supplied by the Swedish manufacturer Sontech.[4] Microperforated plates under the trade name Acustimet form part of the airborne sound absorption materials group and are available in mild and stainless steel, and aluminum. The perforations are produced by punching rather then drilling; this produces a sharp-edged hole geometry that is extremely difficult to define geometrically. The plate supplied was made of aluminum, and came with the smallest perforation size that the company produces.

One of the most important parameters of the analytical model described in Sec. II is the flow impedance of the microperforated plate. Unfortunately, the manufacturer does not provide such data. Manufacturers rarely provide this quantity, but prefer to use the absorption coefficient. However, whereas one can calculate the absorption coefficient from the flow impedance if the configuration is known, one cannot calculate the flow impedance from the absorption coefficient. The starting point in the investigation was thus to determine the flow impedance of the given plate.

One possibility might be to use a set of relationships derived by Maa.[5] Maa's equations are the result of an analysis where the microperforated plate is treated as a lattice of short narrow identical tubes with a certain diameter and a length equal to the thickness of the plate. However, the concept of diameter and thickness cannot be attributed to the punched perforations in the Acustimet plates, since each hole has a unique geometry with sharp edges that protrude out of the surface of the plate. Accordingly, it was decided to determine the flow impedance experimentally.

A widely accepted method of measuring the flow impedance of a perforated plate has been devised by Ingard and Dear.[6] This simple method is known to give reliable results, but it suffers from one major drawback: It gives the flow impedance only at certain discrete frequencies. Ren and Jacobsen have further developed this method to give the flow impedance as a continuous function of the frequency.[7] A sample of the material is placed in an impedance tube driven by a loudspeaker at one end and terminated near anechoically at the other end. Two microphones are mounted on either side of the sample, with their diaphragm flush with the inside surface of the tube. The complex flow impedance is calculated from the measured transfer function between the two microphones. Reflections from the near-anechoic termination, and possible amplitude and phase mismatch of the two microphones are taken into account.[7]

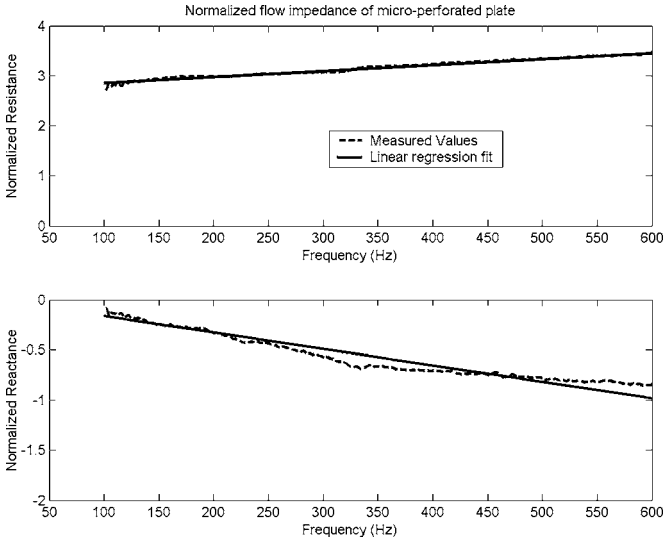

FIG. 3. Real and imaginary part of measured flow impedance of the Acustimet sample, and linear fits. The data are normalized with $\rho_0 c_0$.

A number of different samples were tested using this method, including conventional perforated plates with circular holes of submillimeter size. In general, the results agreed qualitatively and quantitatively well with Maa's theory, according to which the real part of the flow impedance depends weakly on the frequency, whereas the imaginary part is essentially masslike.[5] The method is rather sensitive to how the sample is mounted inside the tube, and leaks and structural vibrations in the sample can be difficult to eliminate completely. However, errors due to these effects dominate only at specific frequencies and a linear regression fit can be used to retrieve the general trend. Figure 3 shows the flow impedance (real and imaginary parts) and corresponding linear approximation of the Acustimet sample used for the experimental validation of the theoretical model described in Sec. II. The results are normalized by $\rho_0 c_0$. The holes in this 1-mm-thick sample can be considered to be slits approximately 3.5-mm long and 0.2-mm wide. The fractional open area was estimated at 2–3 %; this explains the relatively high impedance values.

B. Green's function in a cavity with a microperforated plate

A set of experiments were carried out in a rectangular cavity with dimensions of 2, 1.2, and 0.2 m; see Fig. 4. These dimensions correspond to the x, y, and z coordinates as defined in Fig. 2. The dimensions of the cavity were chosen such that below 850 Hz, the cavity acts as a two-dimensional space; and the frequencies at which the first modes occur are reasonably spaced apart. The cavity was constructed of 22-mm fiberboard panels screwed and glued together, except for the front vertical panel, which was removable so to allow easy access to the inside of the cavity.

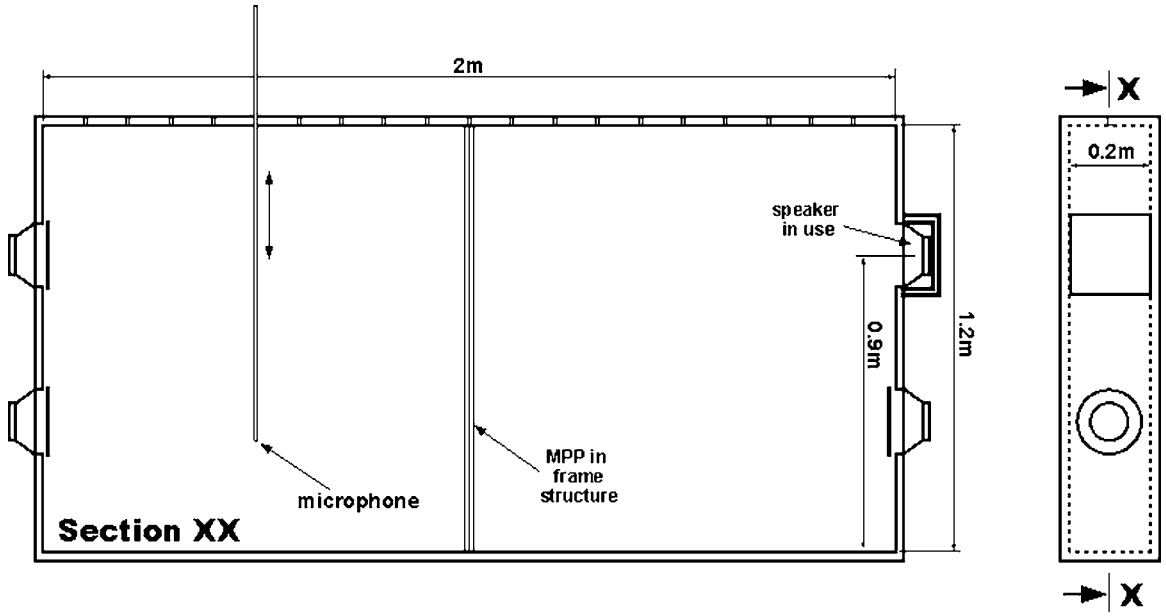

FIG. 4. The flat rectangular cavity used in the experiments. The volume velocity of the loudspeaker that drives the cavity is deduced from the sound pressure in a small box enclosing the back of the loudspeaker. Three unused loudspeakers from an earlier experiment are covered by aluminum plates.

Acoustic modes inside the cavity were excited using white noise generated by a loudspeaker with a diameter of 9 cm mounted on one of the vertical side panels. Pressure measurements inside the cavity were taken through holes in the top panel using an electret microphone with a diameter of 10 mm mounted on the tip of a 1.2-m-long rod. This setup made it possible to measure at a grid of points inside the cavity, so that given a sufficient amount of data points, the mode shape at a particular frequency could be reconstructed. Data was acquired using Brüel and Kjær's "Pulse" front-end and software, which was also used to carry out the fast Fourier transform (FFT) analysis. To get the Green's function the sound pressure data was normalized with the density of air and the volume velocity of the loudspeaker Q, estimated from the sound pressure p_c measured in a small box enclosing the back of the loudspeaker

$$p_c = -Q\frac{\rho_0 c_0^2}{i\omega V_c}, \tag{23}$$

where V_c is the volume of the small cavity, 1100 cm^3; in other words, the Green's function was estimated using the expression

$$G(\mathbf{x},\mathbf{y};\omega) = \frac{p(\mathbf{x})}{-i\omega\rho_0 Q(\mathbf{y})} = -\frac{p(\mathbf{x})}{p_c}\left(\frac{c_0}{\omega}\right)^2\frac{1}{V_c}. \tag{24}$$

When a microperforated plate is mounted inside a cavity driven by a sound source, vibrations of the plate are likely to occur. Such vibrations obviously affect the relative velocity of the air oscillating through the perforations, resulting in an unpredictable damping behavior. To avoid such problems the microperforated plate of dimensions 1.2×0.2 m was clamped between two wooden frames. This arrangement raised the first fundamental structural frequency of the plate from about 60 Hz to above 500 Hz. Although this arrangement may have introduced some level of distortion in the sound field very close to the plate, the necessity of a stationary plate was given higher priority. In what follows the measured flow impedance of the plate has been corrected for the area covered by the supporting frame.

The sound pressure was measured at various locations inside the cavity. Three sets of measurements were taken: a reference measurement without the microperforated plate, and two with the plate mounted at two different positions, in the middle (at $d=1.0$ m, cf. Fig. 2) and close to one side (at $d=0.25$ m). With the plate in the middle it was expected to be easy to distinguish between affected and undamped modes. Modes with $l=1,3,5,\ldots$, should be significantly damped (maximum velocity through plate), while modes with l even should be practically undamped (velocity node at plate). For the third case, with the plate mounted close to one side, the constants i and j as defined in Sec. II B compute to 1 and 7, which implies that the plate has no effect on modes with $l=8,16,\ldots,$. These modes are not present below 500 Hz. It follows that all modes occurring with this setup should be damped with the exception of modes with $l=0$.

For more accurate comparisons between predictions and measurements, Eq. (10) was modified to take into account the finite size of the source (approximated by a square piston with the same area), and the inherent damping of the cavity, which turned out not to be negligible. The latter quantity was estimated from the reverberation time measured in one-third octave bands without the microperforated plate in the cavity.

The reverberation time was found to be approximately 0.5 s in most of the frequency range of concern—which is about one order of magnitude shorter than the reverberation time predicted from viscothermal losses assuming perfectly rigid walls.[8] (One-third octave bands were chosen because one cannot measure short reverberation times with fine frequency resolution.[9]) The corrected expression is

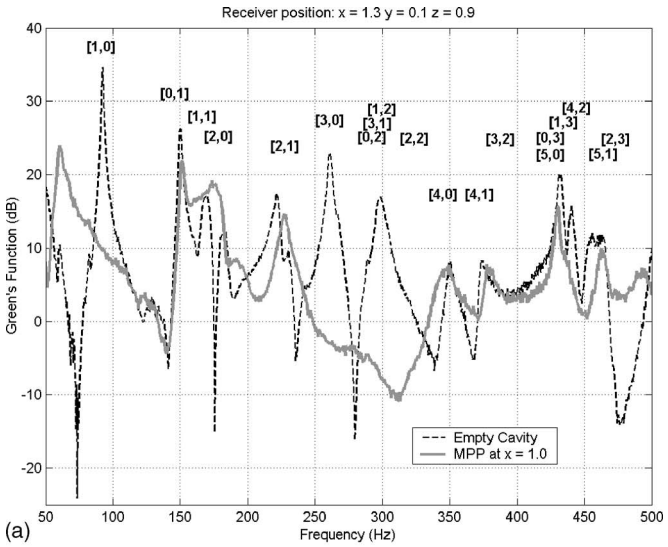

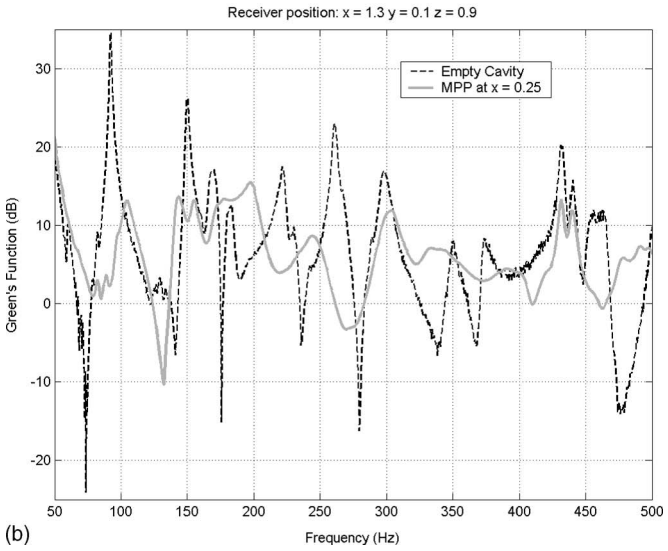

FIG. 5. Measured effect of a microperforated plate mounted (a) in the middle of the cavity, and (b) near a wall.

$$G(\mathbf{x},\mathbf{y};\omega) \approx -\sum_{n=1} \frac{1}{S_{\text{piston}}} \int_{\Xi} \xi_n(\mathbf{y}) \mathrm{d}^2\mathbf{y} \times \frac{\xi_n(\mathbf{x})}{V\left[k_0^2 - \kappa_n^2(\omega) + ik_0 \frac{1}{\tau_n c_0}\right]}, \tag{25}$$

where Ξ denotes the surface of the source with surface area S_{piston}, and τ_n is a modal time constant that takes account of the inherent damping of the enclosure.

A comparison between the measured data in the three different scenarios is shown in Fig. 5. To facilitate mode identification, analytically calculated eigenfrequencies for an empty rigid-walled cavity with the same dimensions are given in Table I and indicated in Fig. 5(a). The particular receiver position used for these results was chosen because it picks up most of the acoustic modes in the given frequency range, but similar results have been obtained at a number of positions. One can immediately notice that the microperforated plate does provide significant damping for particular

TABLE I. Eigenfrequencies of the empty cavity.

l, m	0 (Hz)	1 (Hz)	2 (Hz)
0		143	286
1	86	167	298
2	172	223	333
3	257	294	385
4	343	372	446
5	429	452	

modes. In Fig. 5(a) modes $(1,0)$, $(1,2)$, $(1,3)$, $(3,0)$, and $(3,1)$ are no longer apparent, resulting in attenuations of as much as 25 dB, whereas modes with $l=0,2,4$ as expected are practically unchanged. With the plate close to the side, as shown in Fig. 5(b), the entire Green's function is significantly damped. This includes mode $(0,1)$ (with wave motion parallel to the plate), in disagreement with the theory.

Figure 6 compares experimental data with results predicted using the analytical model described in Sec. II. The

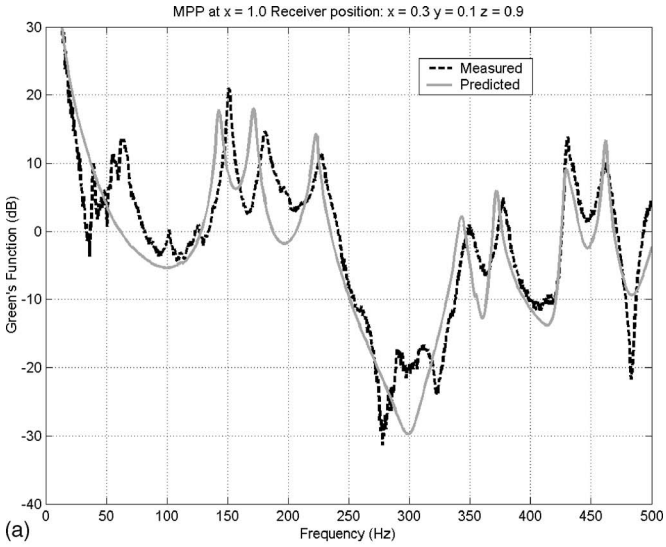

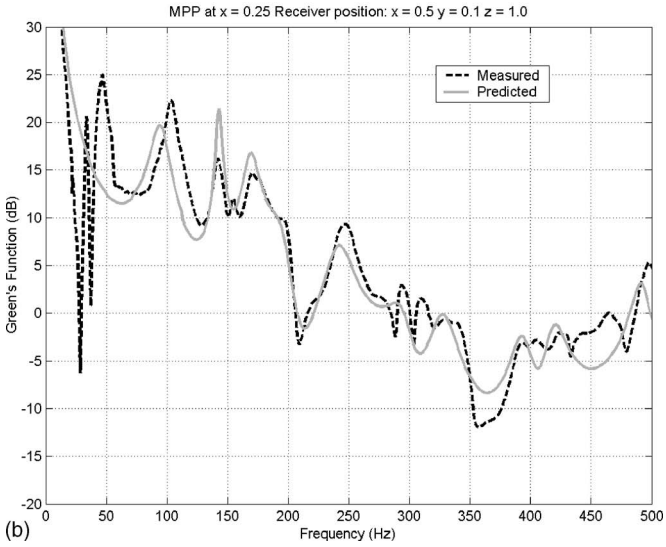

FIG. 6. Measured and predicted Green's function with the microperforated plate mounted (a) in the middle of the cavity, and (b) near a wall.

number of modes summed in the x, y, and z directions are 46, 20, and 3, respectively. Figure 6(a) shows the comparison for the plate in the middle, and Fig. 6(b) shows the case with the plate close to one of the sides of the enclosure. In general, a reasonably good match can be observed in both plots, and the same trends are observed at other locations inside the cavity (not shown).

C. Discussion

The experimental arrangement is not perfect. The most conspicuous difference between predictions and measurements is the small frequency shift between the curves. After extensive testing, this phenomenon has been attributed to vibroacoustic interactions between the sound field inside the cavity and the cavity walls. Such interactions are usually of a very complex nature, and any attempts to take them into consideration in the analytical model would give rise to unnecessary complications. This phenomenon also explains the peaks picked up by the measurements at around 50 Hz, a frequency that is significantly below the first acoustic mode of the cavity (cf. Table I). There are also discrepancies between the magnitudes of the peaks of some modes. In most cases these discrepancies can probably be attributed to the fact that the inherent damping of the cavity was measured in one-third octave bands. Thus if two modes were present in the same one-third octave band, an average decay rate was assumed. Moreover, the vibroacoustic losses of the cavity may have been affected by the introduction of the plate. Yet another source of uncertainty is that the wooden frame supporting the plate changes the geometry of the two subcavities. However, the geometry of the holes of the Acustimet plate is probably the most serious problem. Given their three-dimensional shape, which is almost like that of a grater, it seems reasonable to expect the Acustimet plates to provide damping even to modes with wave motion only parallel to the plate. In all probability this explains the damping of mode $(0,1)$, occurring approximately at 150 Hz. According to the model the $(0,1)$ mode of the empty cavity (with wave motion tangential to the plate) is simply not affected by the plate since, in steady state, the $(0,1)$ modes in the two subcavities match each other exactly so that there is no pressure drop across the plate and therefore no losses. In other word, in such cases the model is conservative and underestimates the damping, as demonstrated in Fig. 6(b).

There seems to be a certain similarity between the behavior of the Acustimet plate and bulk-reacting absorbers; in both cases a normal incidence measurement does not provide sufficient information for predicting the behavior for incidence at arbitrary angles. However, there is also a significant difference between these two cases. In a bulk-reacting absorber there is wave propagation in the material.[10] The effect of a bulk-reacting lining can be determined from equations expressing the boundary condition of the surface of the material (continuity in the pressure and the normal component of the particle velocity) if the characteristic impedance and propagation constant of the material are known.[10,11] By contrast, a strict analysis of the effect of the Acustimet plate seems to involve coupling the regions on either side of the plate through continuity in the pressure and a nonperpendicular component of the particle velocity (or introducing a tensorial flow impedance), and that would be exceedingly complicated.

Nevertheless, in spite of all these shortcomings, the experiments certainly confirm the practical utility of the theoretical approach presented in Sec. II.

IV. CONCLUSIONS

An analytical method for predicting the attenuation provided by a microperforated plate in a cavity has been presented. The microperforated plate is described in terms of its complex flow impedance. The method involves finding complex eigenvalues and eigenfunctions, and is based on solving an eigenvalue equation iteratively using the set of eigenvalues of the cavity with no perforated plate as starting guesses. Each of the resulting eigenvalues corresponds uniquely to an eigenvalue of the cavity without the plate, although the ordering may change.

The model has been validated experimentally by comparing predicted Green's functions with measurements with a microperforated plate mounted in a flat box and using experimentally determined values of the flow impedance of the plate. Very good agreement was obtained, except for one mode with wave motion only parallel to the perforated plate. Because of the peculiar geometry of the punched holes such modes are actually attenuated by the plate, but since the model takes account only of the normal component of the acoustic particle velocity this attenuation is underestimated. However, in general the substantial attenuation provided by the microperforated plate was predicted very well. The model makes it possible to optimize the position of the plate.

These findings show that microperforated plates can provide useful and predictable attenuation of boiler tones in heat-exchange cavities. Further research is underway to determine, in general, the optimal location and flow impedance of a perforated plate for a given cavity geometry, gas temperature, and gas pressure.

ACKNOWLEDGMENTS

The authors would like to thank Ralf Corin at Sontech NoiseControl for providing the microperforated plates used in this project, and also Aage Sonesson and Jørgen Rasmussen, Acoustic Technology, Ørsted-DTU, for their help with the practical aspects of the experimental work.

[1] R. D. Blevins, *Flow-Induced Vibrations* (Wiley, New York, 1990).
[2] G. M. Keith, "Flow-acoustic interactions in heat-exchange cavities. A summary of results and conclusions from recent analyses and experiences." Technical Report, Ødegaard & Danneskiold-Samsøe A/S, 2004.
[3] P. M. Morse and K. U. Ingard, *Theoretical Acoustics* (McGraw-Hill, New York, 1968).
[4] Sontech Noise Control, Airborne sound absorption: Acustimet. http://sontech.se
[5] D.-Y. Maa, "Potential of micro-perforated panel absorber," J. Acoust. Soc. Am. **104**, 2861–2866 (1998).
[6] K. U. Ingard and T. A. Dear, "Measurement of acoustic flow resistance," J. Acoust. Soc. Am. **103**, 567–572 (1985).
[7] M. Ren and F. Jacobsen, "A method of measuring the dynamic flow resistance and reactance of porous materials," Appl. Acoust. **39**, 265–276 (1993).

[8]L. Cremer and H. A. Müller, *Principles and Applications of Room Acoustics*, Vol. **2** (Applied Science Publishers, London, 1978). See Sec. IV.7.8 "Unavoidable sound absorption at a rigid wall."
[9]F. Jacobsen, "A note on acoustic decay measurements," J. Sound Vib. **115**, 163–170 (1987).
[10]F. P. Mechel and I. L. Vér, "Sound absorbing materials and sound absorbers," in *Noise and Vibration Engineering: Principles and Applications*, edited by L. L. Beranek and I. L. Vér (Wiley, New York, 1992), Chap. 8.
[11]R. A. Scott, "The propagation of sound between walls of porous materials," Proc. Phys. Soc. **58**, 358–368 (1946).